MOGA OPTIMIZATION DESIGN OF LCLS-II LINAC CONFIGURATIONS*

L. Wang[#], P. Emma, Y. Nosochkov, T. Raubenheimer, M. Woodley and F. Zhou,
SLAC, Stanford, CA 94309, USA
C. Papadopoulos, J. Qiang and M. Venturini, LBNL, Berkeley, CA 94720, USA

Abstract

This paper briefly summarizes the preliminary optimization study on the configurations of LCLSII with superconducting cavity. The setup of each configuration is first optimized using Multi-Objective Genetic Algorithm (MOGA) with LiTrack which includes the longitudinal phase space only. For each operation mode, MOGA is applied to optimize the machine parameters in order to get flat top current profile and zero energy chirp at the beginning of the undulator. The geometric wake of the RF cavities and resistive wall wake of the beam pipe are included, but the coherent synchrotron radiation (CSR) wake is not included. Finally, ELEGANT code is used to do full 3-dimension particle simulation, which includes the CSR and ISR effect. Therefore, the emittance growth due to CSR can be checked. A new code has been recently developed to integrate all the wake field and CSR in the MOGA optimization.

INTRODUCTION

The new LCLS-II high-repetition rate FEL project at SLAC [1] will use a new superconducting linac composed of TESLA-like RF cavities in continuous wave (CW) operation, in order to accelerate a 1-MHz electron beam to 4 GeV. Figure 1 shows the optics (top) of the hard x-ray beam and the layout of LCLS-II linac(bottom). The new superconducting linac is driven by a new high-rate injector [2], will replace the existing SLAC copper linac in sectors 1-7 (101.6 m/sector), while the remaining Cu RF structures in sectors 7-10 will be removed and replaced with a simple beam pipe and focusing lattice (the "linac extension"). The existing 2-km PEP-II bypass line (large β section in Fig.1) will be modified to transport electrons from the linac extension in sector 10 through more than 2.5 km and into either of two undulators in the existing LCLS undulator hall. The overall design of the linac can be found in [3]. The resistive wall wake field along this long bypass beam line play an important role in the linac design as discussed later. The current design has two bunch compressors (BCs), which are located at the 2nd and 3rd non-zero horizontal dispersion sections in Fig. 1. The 1st dispersion section is laser heater. The injector beam is optimized at beam energy of 98MeV [4] to give a small transverse emittance and certain peak current. This paper describes the optimizations afterwards to the beginning of the FEL undulator.

The main parameters to be optimized include the phase and voltage of linac 1 (L1), linearizer (before BC1), linac 2 (L2) (between BC1 and BC2) and the R56 of BC1/BC2.

The beam energies at BC1 and BC2 are 250MeV and 1.6GeV, respectively. The beam is accelerated to 4.0 GeV by linac 3 (L3).
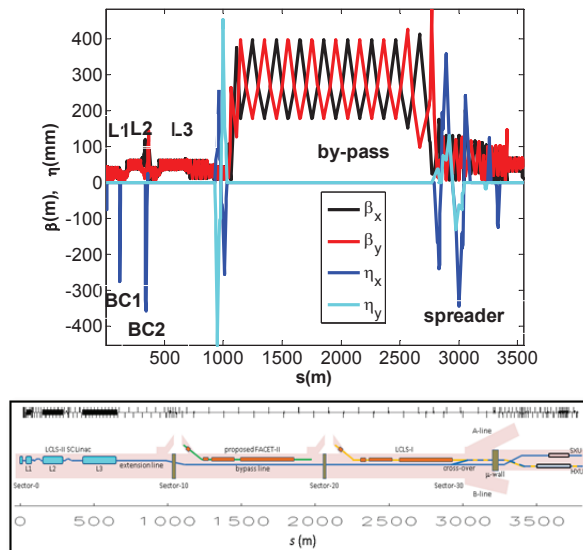

Figure 1: Optics (HXR)(top) and Layout (bottom) of the LCLS-II linac. The BC1 and BC2 are located at the 2nd and 3rd non-zero horizontal dispersion section, respectively.

NONLINEAR BEAM FROM INJECTOR

In the current design, the injector of LCLS-II uses CW normal conducting RF gun [2]. The strong space charge effect at the injector induces large nonlinearity in the longitudinal phase space. The dominant one is cubic term, which is the fundamental term of the longitudinal space charge effect. The high order terms also have large contributions to the linac beam dynamics. These nonlinear effects are amplified throughout the linac when the bunch is compressed. The strong space charge effect makes LCLS-II beam largely different from the existing LCLS beam where the nonlinear term (cubic term dominant) is mainly induced by the strong geometric wake in the normal conducting RF structures. As a result, the design of LCLS-II beam has strong dependence on the injector.

The longitudinal phase space, current profile and
$$Bmag = 0.5\left(\frac{\beta_0}{\beta} + \frac{\beta}{\beta_0} + \left(\alpha\sqrt{\frac{\beta_0}{\beta}} + \alpha_0\sqrt{\frac{\beta}{\beta_0}}\right)^2\right)$$
along the bunch at linac with 98MeV beam are shown in Fig. 2 for three bunch charges: 20pC, 100pC and 300pC. The overall bunch profile is similar: there is a long bunch tail. The nonlinearity can be clearly seen after extracting the linear chirp and RF curvature as shown in Fig. 3. The high order terms are comparable to the cubic term. The

nonlinearity is about proportional to the peak current. A 20pC bunch charge with 10A peak current has too large nonlinearity, which makes it difficult to provide good quality beam for FEL. For this reason, a lower peak current of 4.5A is chosen for 20pC to reduce the space charge effect.
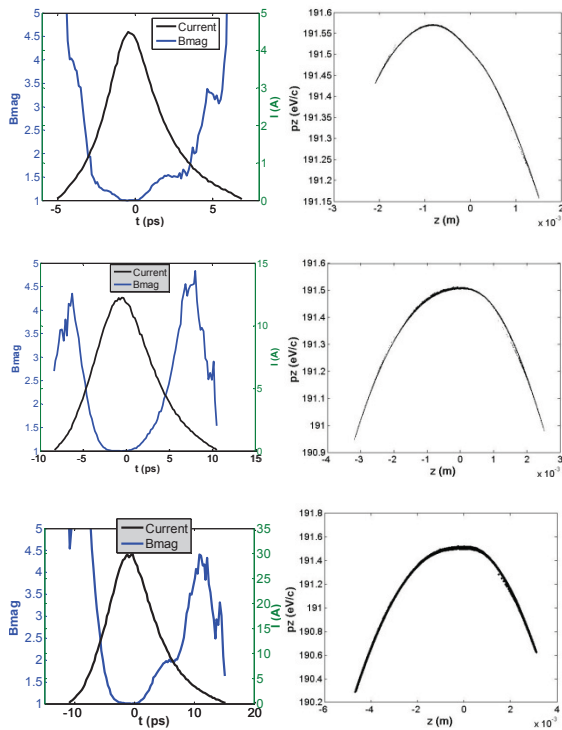

Figure 2 : Current profile (left) and Phase space (right) at the exit of injector linac (98MeV) for 20pC (top), 100pC (middle) and 300pC (bottom) bunch charge. Bunch head is to the left.

The strong space charge also causes mismatching along the bunch, especially for 20pC case where the space charge is stronger. However, the core bunch still has good matching. When the beam passes through the linac, the collective effects add more mismatching to the beam. The mismatched beam can affect the FEL performance [5,6].

STRONG RESISTIVE WALL WAKE AS A NATURAL DE-CHIRPER

The wake fields play an important role in the beam dynamics: de-chirper the beam and increase the nonlinearity.

Figure 4 shows the longitudinal wake in the 1.3GHz and 3.9GHz SC cavity, which is used to linearize the phase space before BC1. The linearizer has much stronger wake.

On the other hand, the resistive wall (RW) wake plays an important role to de-chirper the beam. Table 1 lists the contributions of the resistive wall wake, which is dominant by the 2km-long bypass line. The beam is chirped along Linac 1 and Linac 2 by the RF cavities in order to compress the beam. This positive chirped beam is naturally de-chirped by the resistive wall wake after Linac
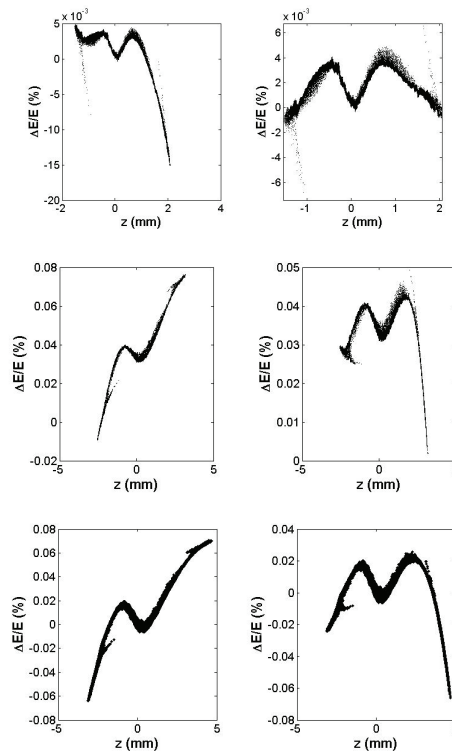

Figure 3 : 3rd-order term (left column) and high order terms (right column) at the exit of injector linac (98MeV) for 20pC (top), 100pC (middle) and 300pC (bottom) bunch charge.

3 if the design is optimal. This is a nice feature of LCLSII design. However, this also puts a strong constraint on the design since the RW wake field cannot be adjusted. The large de-chirp effect due to the resistive wall wake requires enough chirper to be provided by the RF cavities. For 1kA peak current of flat beam, the energy loss due to the resistive wall wake are 4.8MV, 18MV and 34MV for 20pC, 100pC and 300pC, respectively. Figure 5 shows the evolution of longitudinal phase space where the de-chirper by the RW wake is clear seen.

The strong de-chirp of RW wake sets a tight constraint in the linac design. It is too strong for high charge so that it leads to a large bunch compression factor at the second bunch compressor, and therefore a large R_{56}. In most cases, there is no need for additional de-chirper. Instead, it requires the linac RF to provide large enough energy chirp to compensate the RW effect, which adds a constraint in the set-up of the bunch compressor systems. Indeed, the design of the BCs strongly depends on the RW wake. The design has more flexibility for a small RW wake.

Besides the energy loss due to the resistive wall wake, the RW wake also can spoil the phase space. The nonlinear wake field for a longer bunch (>100μm) causes strong distortion in phase space. This makes it difficult to provide high quality long bunch, for instance, 300pC bunch charge with peak current 500A. The RW wake with Aluminum pipe has stronger nonlinearity and it would be good to replace it with stainless steel material or surface

coating. Furthermore, when the beam has strong double horn in current profile, the RW wake also induces strong nonlinear de-chirper.
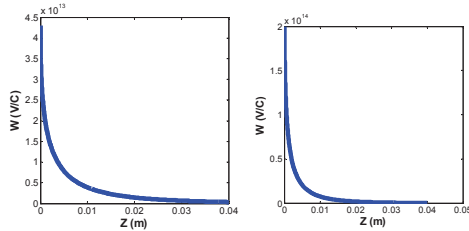

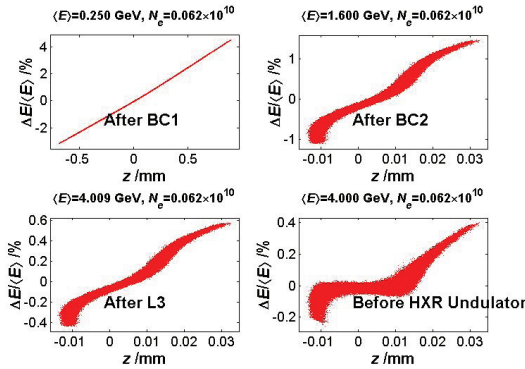Figure 4: Longitudinal wake field in the 1.3GHz (left) and 3.9GHz (right) cavities.

Figure 5: Longitudinal phase spaces for 100pC 1kA beam.

VARIOUS CONFIGURATIONS OF THE LINAC

The fast speed of Litrack code is used in the MOGA optimization [7] in this section. The CSR is not included. Table 2 summarizes the main parameters of the optimized configurations. The strategy of the optimization aims to reduce the RF power while providing a similar beam quality: flat current profile and smaller energy spread (zero energy chirper). A new baseline, which tends to reduce the R56 at BC2 by increasing the compression factor at BC1 in order to mitigate the CSR at BC2, is also added in Table 2 to show the range of the parameters. It uses a reduced RW wakes compared with the one listed in Table 1.

The energy losses due to CSR at BC2 are also listed in the Table (detail see next section). The power is calculated for a repetition rate of 929 kHz for all bunch charges. The energy loss in BC1 is about 1W for 100pC and 3W for 300pC. The maximum power loss in BC2 is about 117 W for 300pC charge, which can become even larger when larger peak currents are applied in the future.

Figure 6 shows the phase space and current profile at the beginning of the undulator by Litrack. The current profiles are all flat except 100pC 1.5kA case. These flat current profiles are essential for the self-seeding. There are also always near zero energy chirp for the core part of bunches.

Table 1: Resistive Wake along the Linac

Beam line Section	Pipe Length(m)	Pipe Radius(mm)	Material	Conductivity (Ohm-m)	Time Constant (fs)	Peak Energy Loss (MeV)
Linac Extension	353	24.5	S.S	1.37×10^6	5	1.2
Rolled DogLeg #1	50	12.7	S.S	1.37×10^6	5	0.5
Bypass Line	2193	24.5	S.S	1.37×10^6	5	12.06
DL&LTU to Und.	382	12.7	AL	3.60×10^7	5	4

Table 2: Configurations for BC1 Energy 250MeV and BC2 Energy 1.6GeV, without Dechirper

|	20pC, 500A	100pC, 1kA	100pC, 1kA, New baseline [3]	100pC,1.5kA	300pC, 1kA	300pC, 600A
$\phi_{L1}(°)$	-21	-21	-12.2	-21.9	-19.85	-20
$\phi_{Linearizer}(°)$	-165	-165	-150	-164.5	-162.2	-162
$\phi_{L2}(°)$	-21.1	-21	-21.1	-28.4	-28.86	-29
$\phi_{L3}(°)$	0	0	0	0	0	0
V_{L1} (MV)	219.6	219.6	216	225	222	222
$V_{Linearizer}$ (MV)	54.78	54.78	64.90	58.7	59.58	59.58
BC1 R_{56} (mm)	-53	-55	-55	-53.46	-47.4	-44.7
BC2 R_{56} (mm)	-61.8	-60	-37.5	-45.5	-49.2	-49.2
σ_{z0} (mm)	0.627	1.02	1	1.02	1.30	1.30
I_{pk0} (A)	4.5	12	12	12	31	31
σ_z^{BC1}(mm)	0.187	0.283	0.15	0.246	0.43	0.48
I_{pk}^{BC1} (A)	15	43	82	50	91	82
σ_E^{BC1}(%)	0.835	1.36	1.6	1.469	1.857	1.857
σ_z^{BC2}(μm)	5.16	8.85	9.2	5.516	29	48
I_{pk}^{BC2} (kA)	0.515	1.355	1.36	2.723	1.18	0.75
σ_E^{BC2}(%)	0.295	0.458	0.378	0.53	0.822	0.884
σ_E^{UndBEG}(%)	0.055	0.065	0.066	0.079	0.239	0.346
$P_E^{BC2CSR}(W)$		42		88	117	84
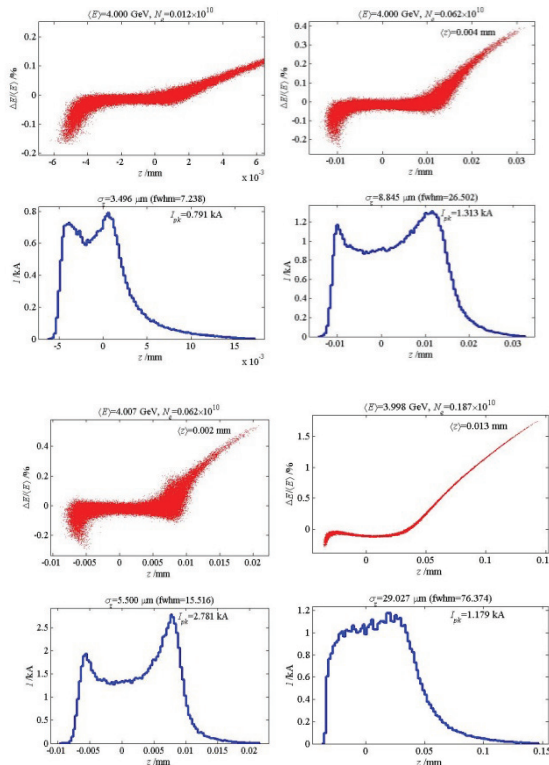
Figure 6: Phase space and current profile before the undulator for different configurations (from top/left to bottom/right: 20pC@500A, 100pC@1kA, 100pC@1.5 kA, 300pC@1kA).

CSR EFFECT ON THE BEAM

After getting satisfactory solutions from MOGA optimization, we use ELEGANT to track particles 3-dimensionaly. Besides the wake fields, the CSR and ISR are included. The CSR changes the beam current profile and some parameters are tweaked to get flat top current profile.

BC1 and BC2 are located along the Superconducting Linac. Therefore, the energy loss there due to CSR needs to be evaluated. The energy loss due to CSR at the 2nd bunch compressor (BC2) is large due to the high peak current there. The radiation can propagate to the downstream and heat the superconducting RF cryomodule. The ISR in general is much smaller compared with the CSR. Unlike a true wake, each particle is affected only by those behind it. Also unlike true wakes, the effects of CSR depend on the slope of the bunch distribution. The steady status CSR model largely underestimates the CSR since the bending magnets are short in our case.

The reality of CSR in a bunch compressor is much more complicated than the 1-D steady state result. The transient effects entering bend magnets and the propagation of CSR through drifts following the bending magnets and the variation of bunch profile are all important. Furthermore, the CSR affects the transverse dynamics throughout the bunch compressor where the

transverse beam size and beam optics vary. The estimation of CSR in the paper includes all above factors by tracking the particles through the bunch compressors. The total energy loss at BC2 for various configurations is listed in Table. 2.

Figure 7 shows total CSR kicker along the bunch through BC2 for 300pC. The energy loss is up to 0.7MeV. The CSR kicker in this case acts like a linear de-chirper for the core part of bunch. However, when the bunch profile is not flat, the CSR kicker has strong nonlinearity.

Figures 8-11 shows the longitudinal phase space and current profile at the beginning of the undulator for various configurations. The simulations are done with ELEGANT code which includes the geometric wake fields, resistive wakes, ISR and CSR. The CSR has large impact on the beam. For instance, the current profile with CSR is different from the ones without CSR as shown in the previous sections. The phase space can also vary a lot due to the CSR. It is better to optimize the beam with CSR so that the solutions are the final ones.

The CSR can increase the projected emittance. The configuration of 300pC bunch charge with 700A is very good, which has zero emittance growth. The 20pC beam also has very small emittance growth. Figure 12 shows the slice emittance of 100pC 1kA beam and 300 pC 1kA beam. The emittance growth for 100pC charge 1kA beam is very small. However, the emittance at head of bunch for 300pC 1kA bunch is spoiled by CSR in the spreader (at 3000meter in Fig. 1). This emittance growth can be minimized by optimizing the optics there. We haven't applied any emittance cancellation schemes [8-11] yet. Overall, the emittance growth can be controlled by optimizing the current profile, reducing R56 and applying cancellation schemes.
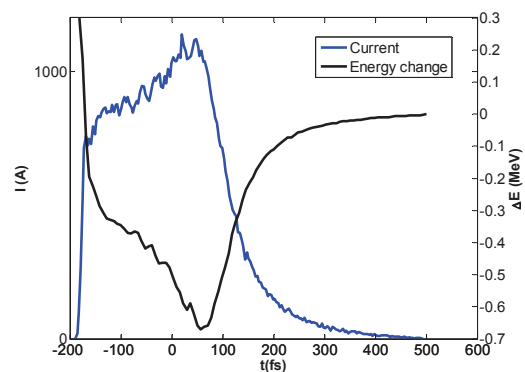

Figure 7: Energy loss due to CSR at whole BC2 for 300pC beam. The bunch shape is also shown, with the head to the left (the blue curve).
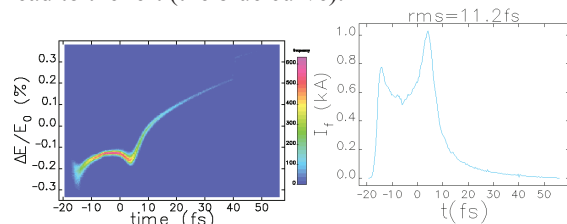

Figure 8: Phase space before undulator from Elegant simulation for 20pC beam with 600A peak current.
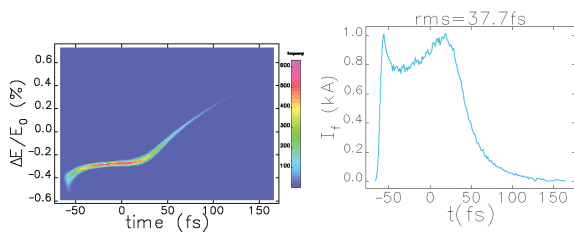
Figure 9: Phase space before undulator from Elegant simulation for 100pC beam with 1.0kA peak current.
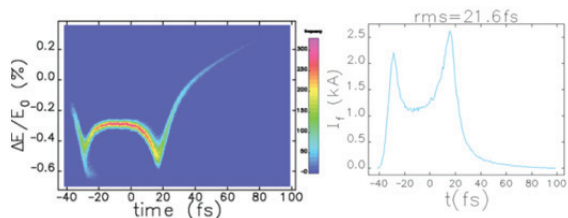

Figure 10: Phase space before undulator from Elegant simulation for 100pC beam with 1.5kA peak current.
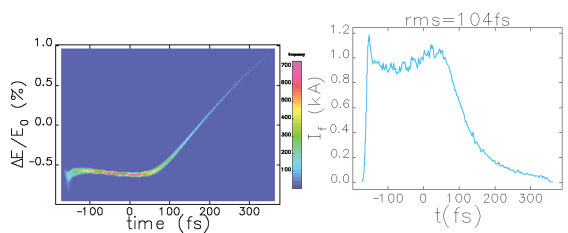

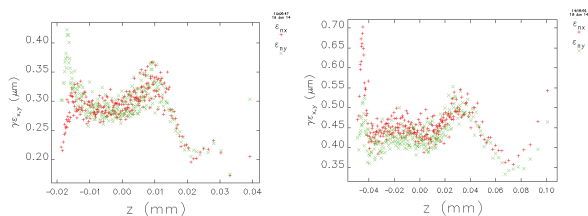Figure 11: Phase space before undulator from Elegant simulation for 300pC beam with 1kA peak current.

Figure 12: Slice emittance at the beginning of undulator for 100pC 1.0kA (left) and 300pC 1kA (right).

TOWARDS HIGH PEAK CURRENT

Preliminary study shows that it is a bit of a challenge to set-up high peak current configuration. Besides the projected emittance growth due to CSR, the large energy loss can distort the phase space. The emittance growth can be mitigated or cancelled by optics design, however, there is no simple mitigation for the latter. For instance, the peak current at 20pC can be easily above 3kA. Figure 13 shows an example of the ELEGANT simulation. However, the collective effect largely distorts the phase space. This makes the high peak current configuration difficult.

A new program is recently developed to include the CSR in the MOGA optimization. The studies show we are able to increase the peak current more than 1kA as what we have now. Figure 14 shows one example of the preliminary result for 300pC. A peak current of 1.5kA

with flat current profile is achieved, which is much better than the 1.5kA beam shown in Fig. 6 where there is a large horn in the current profile. Further careful studies including the emittance growth are under the way.
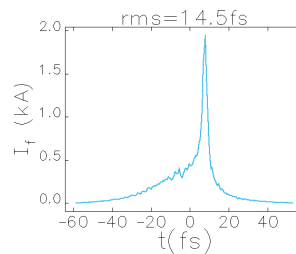

Figure 13: Current profile of 20pC bunch before the Undulator. Elegant simulation.
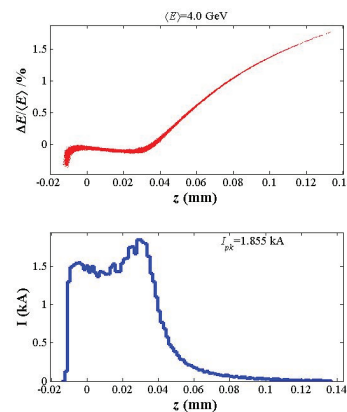

Figure 14: Example of high peak current solution for 300pC charge. Wake fields and CSR are included.

SUMMARY AND OUTLOOK

MOGA is applied to optimize the LCLSII in order to get flat top current profile and zero energy chirp. Small energy spread, zero energy chirp and flat current profile are achieved for different bunch charges. MOGA provides a very useful tool in the design.

One kA flat beams with good emittance are obtained for both 100 pC and 300 pC bunch charge. 20pC bunch has very small emittance, however the peak current with a flat current profile is below 1kA. Although a single spike with high peak current (>2kA) is possible, the beam quality is largely spoiled by the CSR.

In short summary, the resistive wall provides a strong de-chirper and has large impact on the design of LCLSII linac. The new proposed RW wake is about 30% smaller compared to what we used in Table 1 [3]. This allows more freedom in the design. For instance, a smaller compression factor at BC2 (therefore a small R56) is possible. A small R56 reduces the CSR there. However, a large R56 may provide stronger damping to the micro-bunch instability which is a concern now.

The emittance growth due to CSR can be well controlled for 1kA beams. However, the CSR can spoil the longitudinal phase space. Low charge modes are difficult and require more work. It is promising to have a high peak current 1.5 kA with flat current profile.

Studies show that there is a strong micro-bunch instability driven by the longitudinal space charge (LSC) impedance, especially along the long bypass beam line. This may have an impact on the linac design. The studies in this paper haven't included LSC, we are working on it.

ACKNOWLEDGEMENTS

REFERENCES

[1] T. Raubenheimer, "The LCLS-II, a New FEL Facility at SLAC", in Proc. of 36th Int. Free-Electron Laser Conf., Basel, 2014, WEB001.

[2] J. Schmerge et al., "The LCLS-II Injector Design", in Proc. of 36th Int. Free-Electron Laser Conf., Basel, 2014, THP042.

[3] P. Emma, et al., "Linear Accelerator Design for the LCLS-II FEL Facility ", in Proc. of 36th Int. Free-Electron Laser Conf., Basel, 2014, THP025.

[4] C.F. Papadopoulos, et al, "RF Injector Beam Dynamics Optimization for LCLS-II", in Proceedings of IPAC'14, Germany, June 2014, WEPRO015 (2014).

[5] G. Penn, T.O. Raubenheimer, L. Wang, P. Emma, E. Hemsing, Z. Huang, "LASER SEEDING SCHEMES FOR SOFT X-RAYS AT LCLS-II", in Proc. of 36th Int. Free-Electron Laser Conf., Basel, 2014, MOP075.

[6] G. Marcus, Y. Ding, P. Emma, Z. Huang, T. Raubenheimer, L. Wang, J. Wu, "FEL SIMULATION AND PERFORMANCE STUDIES FOR LCLS-II". in Proc. of 36th Int. Free-Electron Laser Conf., Basel, 2014, TUP032.

[7] L. Wang and T. O. Raubenheimer, "Multi-Objective Genetic Optimization for LCLSII X-Ray FEL", Proceedings of FEL 2013, August 2013, p.12(2013); Journal of Mechanics Engineering and Automation 4 (2014) 632-638.

[8] E.L. Saldin, E.A. Schneidmiller, M.V. Yurkov, "On the coherent radiation of an electron bunch moving in an arc of a circle", Instrum. Methods Phys. Res., Sect. A 398, p373 (1997).

[9] D. Douglas, "Suppression and Enhancement of CSR-Driven Emittance Degradation in the IR-FEL Driver", Thomas Jefferson National Accelerator Facility Report No. JLAB-TN-98-012, 1998.

[10] S. Di Mitri, M. Cornacchia, and S. Spampinati, "Cancellation of Coherent Synchrotron Radiation Kicks with Optics Balance", PRL 110, 014801 (2013).

[11] Yichao Jing, Yue Hao, and Vladimir N. Litvinenko, "Compensating effect of the coherent synchrotron radiation in bunch compressors", Phys. Rev. STAccel. Beams 16, 060704 (2013).